Journal of Physics: Conference Series **1342** (2020) 012109 doi:10.1088/1742-6596/1342/1/012109

Thermal management and modeling for precision measurements in Borexino's SOX and solar neutrino spectroscopy programs

David Bravo-Berguño[1]
INFN Sezione Milano, Via Celoria 16, 20133 Milano (Italy)
E-mail: David.Bravo@mi.infn.it

on behalf of the Borexino Collaboration:

M Agostini, K Altenmüller, S Appel, V Atroshchenko, Z Bagdasarian, D Basilico, G Bellini, J Benziger, D Bick, G Bonfini, B Caccianiga, F Calaprice, A Caminata, S Caprioli, M Carlini, P Cavalcante, A Chepurnov, K Choi, O Cloué, L Collica, M Cribier, D D'Angelo, S Davini, A Derbin, X F Ding, A Di Ludovico, L Di Noto, I Drachnev, M. Durero, S Farinon, V Fischer, K Fomenko, A Formozov, D Franco, F Gabriele, J Gaffiot, C Galbiati, M Gschwender, C Ghiano, M Giammarchi, A Goretti, M Gromov, D Guffanti, C Hagner, T Houdy, E Hungerford, Aldo Ianni, Andrea Ianni, N Jonquères, A Jany, D Jeschke, V Kobychev, D Korablev, G Korga, V Kornoukhov, D Kryn, T Lachenmaier, T Lasserre, M Laubenstein, E Litvinovich, F Lombardi, P Lombardi, L Ludhova, G Lukyanchenko, L Lukyanchenko, I Machulin, G Manuzio, S Marcocci, J Maricic, G Mention, J Martyn, R Mereu, E Meroni, M Meyer, L Miramonti, M Misiaszek, V Muratova, R Musenich, B Neumair, L Oberauer, B Opitz, V Orekhov, F Ortica, M Pallavicini, L Papp, Ö Penek, N Pilipenko, A Pocar, A Porcelli, G Ranucci, A Razeto, A Re, M Redchuk, A Romani, R Roncin, N Rossi, S Rottenanger, S Schönert, L Scola, D Semenov, M Skorokhvatov, O Smirnov, A Sotnikov, L F F Stokes, Y Suvorov, R Tartaglia, G Testera, J Thurn, M Toropova, E Unzhakov, C Veyssiére, A Vishneva, M Vivier, R B Vogelaar, F von Feilitzsch, H Wang, S Weinz, M Wojcik, M Wurm, Z Yokley, O Zaimidoroga, S Zavatarelli, K Zuber and G Zuzel

Abstract. Borexino has performed the first direct, high-precision, wideband solar neutrino spectroscopy of the solar neutrino spectrums main components, including improving the knowledge of the CNO ν flux. Its next-generation short-baseline ^{144}Ce-^{144}Pr $\overline{\nu}_e$ source program (CeSOX) intends to unambiguously measure or disprove signs of anomalous oscillatory behavior in the low L/E regime. Both programs rely on the detector's unprecedented and record-setting background levels, which are tightening its requirement for background stability. Aiming to minimize background fluctuations (particularly ^{210}Po), a new Temperature Monitoring and Management System was deployed. Computational Fluid Dynamics (CFD) simulations are also being developed in order to model, characterize and ultimately predict the subtle fluid currents that might be a hindrance for the required background stability.

1. Introduction

The Borexino liquid scintillator (LS) neutrino observatory is devoted to performing high-precision neutrino observations, and is optimized for measurements in the low energy (sub-MeV) region of the solar neutrino spectrum. Borexino has succeeded in determining all major solar neutrino flux components already with its first dataset *Phase 1* (2007-10): first direct detections of *pp* [1], *pep* [2], ^{7}Be [3], and lowest-threshold observation of ^{8}B[4] at 3 MeV, as

[1] Work also developed at previous address: Physics Department, Robeson Hall, Virginia Polytechnic Institute and State University, 24061 Blacksburg (VA) - United States of America

well as the best available limit in the CNO solar ν flux [4]. More recently, high-precision (down to ∼2.8%) determinations of the aforementioned solar neutrino fluxes have been attained using new techniques and enlarged statistics from the post-LS-purification phase: *Phase 2* [5][6]. Geoneutrinos have also been measured with high significance (5.9σ [7]) by Borexino, thanks to the extremely clean $\overline{\nu}_e$ channel –which is expected to gain even more relevance during the *Short-distance neutrino Oscillations with boreXino* (SOX) phase of the experiment. An $\overline{\nu}_e$ generator will be placed in close proximity to the detector during CeSOX, in order to probe for anomalous oscillatory behaviors and unambiguously check for experimental signatures along the phase space light sterile neutrinos might lie in [8] [9]. These results are possible thanks to the unprecedented, extremely radio-pure conditions reached in the Active Volume (AV) of the detector (down to $\leq 10^{-19}$ g(^{239}U/Th)/g(LS) [5]) –achieved thanks to a combination of ultra-clean construction and fluid-handling techniques, as well as dedicated scintillator purification campaigns [10]. Detailed detector response determination was made possible thanks to very successful internal calibration campaigns [11] which did not disturb the uniquely radio-pure environment.

Borexino, located in the Hall C of the Gran Sasso National Laboratories' (LNGS) underground facilities (3,800 m w.e.), measures solar neutrinos via their interactions with a 278 tonnes target of organic liquid scintillator (LS): pseudocumene (PC, or 1,2,4-trimethylbenzene) solvent with 1.5 g/l 2,5-diphenyloxazole (PPO) scintillating solute, contained inside a thin, 8.5m-diameter transparent spherical nylon Inner Vessel (IV). Solar neutrinos are detected by measuring the energy and position of electrons scattered by neutrino-electron elastic interactions converted into electronic signals (photoelectrons or p.e.) by 2,212 photomultipliers (PMT) mounted on a concentric 13.7 m-diameter stainless steel sphere (SSS, see Figure 1). A software-defined Fiducial Volume (FV) is established within the AV. The volume between this IV and the SSS is filled with 889 tonnes of non-scintillating "buffer" (PC+2-3 g/L dimethylphthalate DMP) acting as a radiation shield for external γs and n^0s. The SSS is immersed in a 2,100-tonne Water Tank (WT) used as a Čerenkov detector for residual cosmic $\mu^{\pm}$.

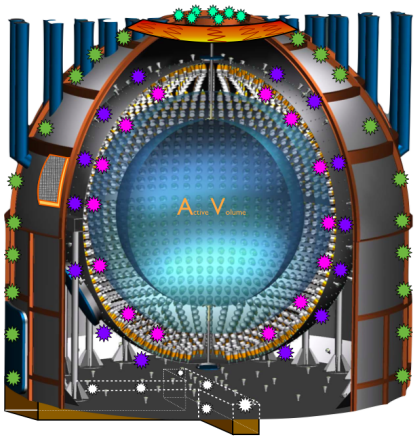

Figure 1. Cutaway of Borexino, featuring the subsystems of the Borexino Thermal Monitoring and Management System (BTMMS): the Latitudinal Temperature Probes System (LTPS, colored stars), a representative section of the Thermal Insulation System (TIS, grey-orange panel on left side of WT) and a conceptual representation of the Active Gradient Stabilization System (AGSS, top orange band). See full text for details. The Active Volume (AV) where the LS is contained is demarcated by the Inner Vessel (IV).

2. Motivation: relation between background and thermal stabilities in Borexino

The unprecedented radiopurity levels reached in Borexino's LS are the key to the uniqueness of the detector's results. The conditions reached after the purification campaign in 2011 [5] mean that mixing of the free scintillating fluid inside the IV could cause unwanted background fluctuations that, with careful management measures, may be minimized or avoided.

Of particular importance to Borexino's future is the effort toward measuring the sub-leading, but crucial, CNO solar neutrino component (≤1% of the Sun's output [12]). Its neutrino recoil spectral shape (endpoint at E_{max}=1.74 MeV) places it under several intrinsic Borexino

backgrounds, in particular ^{85}Kr and ^{210}Bi, whose spectral shapes exhibit a large degree of correlation with the solar neutrino signal –especially so for ^{210}Bi in the ∼400 p.e. energy window, where the CNO rate is briefly expected to be higher than the neighboring, ^{7}Be and *pep* neutrinos (see Figure 2). It is estimated a ⩽10% precision in the determination of the ^{210}Bi concentration in Borexino's FV is needed, during a long enough time period, to collect the very low expected CNO ν counts (∼3-5 cpd/100 tonnes).

Its decay daughter ^{210}Po provides an accurate method for succeeding in this determination. Indeed, ^{210}Po's α decay allows for it to be efficiently tagged out through Pulse-Shape Discrimination (PSD) techniques with very low inefficiencies. Conversely, the β^- decay of bismuth (Q=1160 keV, $t_{1/2}$=5 days) provides an indistinguishable (only statistically-subtractable) signal to $\nu_e - e^-$ elastic scatterings which cannot determine the rate down to the required uncertainty levels, due to the shape degeneracy between the bismuth and solar ν components. Indeed, once legacy out-of-equilibrium ^{210}Po levels have decayed away ($t_{1/2}$=138.4 days), the decay curve would asymptotically reach a plateau baseline corresponding to the secular equilibrium levels of ^{210}Bi. This condition has been close at hand for most of Borexino's *Phase 2* DAQ period –but new out-of-equilibrium, regionally-significant fluctuations in the ^{210}Po levels have prevented reaching it (see Figure 3).

Crucially, it is known ^{210}Pb (parent of ^{210}Bi, $t_{1/2}$=22.3 years, off-threshold-low Q-value) exhibits higher concentrations in the IV, and consequently provides a continuous, "inexhaustible" source of ^{210}Bi-Po. Historically, ^{210}Po fluctuations show a correlation with large environmental temperature excursions in the experimental Hall, hinting at a possible mechanism for replenishment of out-of-equilibrium polonium in the FV: fluid mixing through temperature-driven convection from the AV's periphery around the IV toward the center. Concurrently, the regional homogeneity and stability in ^{210}Bi concentration suggests that the underlying fluid-dynamics are slow enough to prevent most of this isotope to be transported inside the FV faster than it decays, establishing a soft upper limit in radial fluid velocity of $\frac{\mathcal{O}(m)}{\mathcal{O}(2{\cdot}10^6 s)}$ ∼<$5{\cdot}10^{-7}$ m/s.

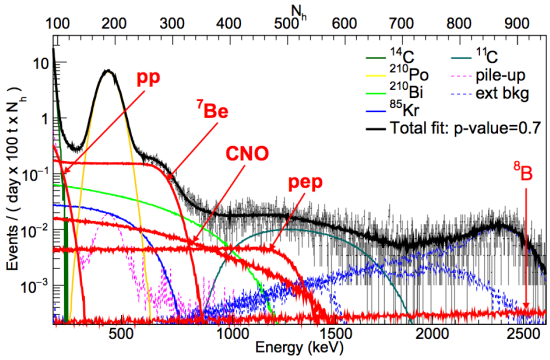

Figure 2. Borexino spectrum in the main analysis energy range (∼500 p.e./MeV), from [5]. Note the near-degeneracy in the ∼850 keV area between ^{210}Bi and CNO ν's spectral shapes, the only window where ν_{CNO} are prevalent over *pp*-chain ν.

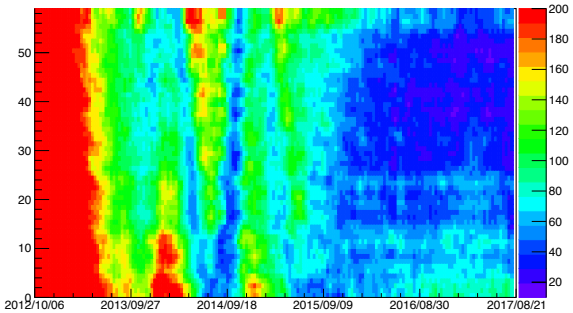

Figure 3. Regional map of historical polonium concentrations (color code: cpd/100 tonnes). Expected plateau levels due to equilibrium ^{210}Bi in the scintillator are ∼20 cpd/100 tonnes. The Y axis indicates regional subdivisions of a 3m-radius FV, running from its bottom to its top.

3. The Borexino Thermal Management and Monitoring System (BTMMS)

Deployment of the three BTMMS subsystems was completed in several periods from 2014-2016:

3.1. Latitudinal Temperature Probes System (LTPS)

Sixty-three custom-calibrated, replaceable, precision temperature sensors installed throughout Borexino provide continuous readings with a finely-spaced, sub-0.05°C relative precision and comparable absolute accuracy [13]. Most of them lie on the same North-South plane (hence "Latitudinal" System), which is useful to contextualize their data. The sensors are grouped in three *"phases"*, based on their location within Borexino: ***Phase I*** comprises 28 sensors installed inside the so-called "re-entrant ports" that connect the exterior to the Outer Buffer (0.5 m inside the SSS for *Phase I.a*'s 14 sensors and 0.5 m outside for *I.b*'s), at SSS latitudes of approximately ±65°, ±50°, ±26° and +7°; ***Phase II*** provides in-plane information on the exterior WT wall (10 sensors, *II.a*) as well as redundant information on different parts of the bottom heat sink (in the SOX pit, *II.b*); and ***Phase III*** corresponds to 7 (*III.a* + *III.b*) sensors on the top of of the detector to monitor its warmest, most thermally-unstable area, as well as two external air monitors (*III.c*). They can be re-calibrated or replaced when needed thanks to their independent, extractable design. The LTPS provides continuous data since as early as November 2014 (Phase I.a) as well as input for numerical fluid-dynamical studies (see Section 4).

3.2. Thermal Insulation System (TIS)

Fully covering Borexino's exterior WT wall and auxiliary structures since late 2015, the TIS comprises two mineral wool layers with an aluminized exterior coating (0.3 W/(m·K), 20 cm thick) that thermally attenuate Borexino's coupling to the exterior environment, limiting thermal disturbances to the interior fluids. It is estimated that ∼60% of seasonal heat transfer is avoided thanks to it, and isotherm divergences from horizontal are also minimized. Phase II.a LTPS sensors are located under it. As a result of the TIS installation (and the shutdown of water circulation in the WT's bottom half), the vertical temperature gradient between Borexino's top and bottom has increased to its historical maximum, stabilizing the vertical fluid stratification to near-equilibrium (see Figure 4), which inhibits convective motions triggering LS mixing.

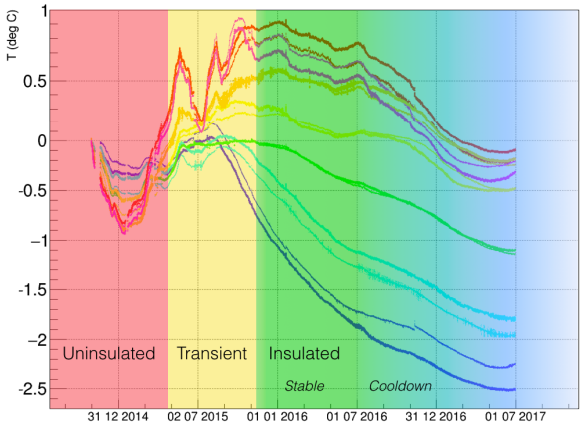

Figure 4. Relative temperature behavior in Borexinos OB from the Phase I.a LTPS, normalized to initial temperature. TIS influence is evident, already since its initial deployment in mid-2015.

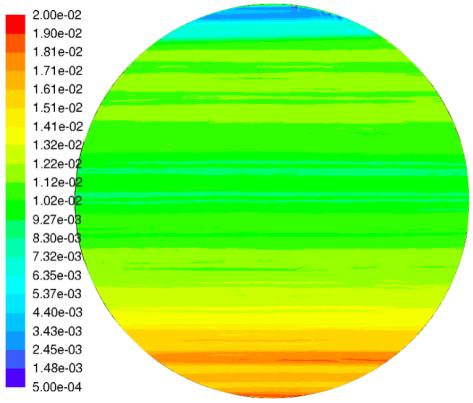

Figure 5. Sample output of a fluid-dynamics simulation of the AV, showing preferential horizontal transport. Color code shows fluid-carrying capacity of each ∼1cm^2 mesh cell, (units: kg/s)

3.3. Active Gradient Stabilization System (AGSS)

A heating system stabilizes temperatures on Borexino's top boundary through a copper serpentine coupled to the top WT dome, under the TIS (monitored by LTPS' *Ph.III.a*). It is

expected to reduce temperature gradient oscillations, avoiding the largest seasonal ΔT's which could trigger strong convection through inward-propagating stratification inversions. It also minimizes the global effects of detector cooling caused by heat loss through the base ($\sim$7°C).

4. Borexino's Computational Fluid-Dynamical (CFD) simulations

Fluid dynamics inside Borexino (especially in its AV) cannot be directly measured beyond its temperature-derived pseudo-stable, positively stratified condition given by the prominent top-bottom temperature gradient. Nevertheless, they are key to reliably understanding the background shifts correlated with temperature excursions (see Section 2) and, in particular, the mechanism behind ^{210}Bi-^{210}Po shifts. For this reason, 2D and 3D CFD models using FLUENT^{TM} [14] and fed LTPS data as boundary conditions have been developed.

They determined several key parameters of Borexino's fluid dynamics, such as: **(i)** conduction-dominated phenomena in whole-detector scales (long-term cooldown due to the TIS, seasonal change extent and speeds with and without insulation, influence of structural heatpaths, boundary effects and power exchange budgeting, etc.); **(ii)** AGSS influence and safe operational range; **(iii)** benchmarks of convection conditions by reproducing representative literature scenarios with similar Rayleigh numbers as in Borexino, as well as a thermal transport benchmark model bounded by *Ph.I.b* data checked through comparison with *Ph.I.a* temperatures in the same OB simulated positions. These benchmarks allowed to determine **(iv)** the leading mechanisms of fluid transport inside Borexino's AV, using a finely-meshed, simple convective model bounded by IV temperatures projected from LTPS' OB data. Challenges to this approach mainly arise, ironically, from Borexino's pseudo-stable fluid condition (long timescales $\mathcal{O}$(months) over large dimensions $\mathcal{O}$(m)), where identifying the model's temporal and spatial granularities is paramount in order to avoid numerical biases overwhelming physical effects

It was found that global transport phenomena are horizontally-dominated, with North-South lateral ΔT asymmetries in isotherms are found to dominate the fluid flow in the AV (see Figure 5). A consistent relationship between the observed simulated currents and the expected ^{210}Bi-Po half-lives constraint (see Section 2) was verified by displacements $\sim \mathcal{O}$(cm-m)/day, validating prior hypotheses. Also, increased top-bottom gradient is seen to limit vertical circulation cell size (if the cells are seen as "pancakes", their thickness) and, with it, the extent of vertical fluid migration inside the bulk of the AV [15].

Current work focuses on clarifying fluid-dynamics' role in ^{210}Po migration, including understanding the role of surface currents as ^{210}Bi reservoirs. Forecasts of probable background distributions in the future are also being actively researched, by quantitatively relating regional polonium concentration to the fluid's local carrying capacity (see Figure 5).

References

[1] Borexino Collaboration 2014 *Nature* **512** 383–386
[2] Borexino Collaboration 2012 *PRL (2012)* **108**
[3] Borexino Collaboration 2011 *PRL (2011)* **107**
[4] Borexino Collaboration 2010 *PRD (2010)* **82**
[5] Borexino Collaboration 2017 *arXiv:1707.09279v1*
[6] Borexino Collaboration 2017 *arXiv:1709.00756*
[7] Borexino Collaboration 2015 *PRD (2015)* **92**
[8] Borexino Collaboration 2013 *arXiv:1304.7721v2 (2013)*
[9] C Giunti etal 2016 *Nucl.Phys.B (arXiv:1512.04758)* **908** 336–353
[10] J Benzinger 2014 *Int.J.Mod.Phys.* **A29**
[11] Borexino Collaboration 2012 *JINST 7 (2012)* **P10018**
[12] N Vinyoles, A M Serenelli, et al 2017 *The Astrophysical Journal* **835**
[13] D Bravo-Berguño 2016 *PhD Thesis, Virginia Tech (2016)*
[14] ANSYS Inc 2016 *User's guide*
[15] DBravo-Berguño and RMereu 2018 *NIM-A 885, 38-53; arXiv:1705.09658*